Ethiopian Journal of Science and Sustainable Development

e-ISSN 2663-3205 *Volume 8 (1), 2021*

Journal Home Page: www.ejssd.astu.edu.et

Research Paper

Medicinal Plant *Syzygium Guineense* (Willd.) DC Leaf Extract Mediated Green Synthesis of Ag Nanoparticles: Investigation of their Antibacterial Activity

Tegene Desalegn[1,*], H C Ananda Murthy[1,*], Yeshaneh Adimasu[2]

[1]*Department of Applied Chemistry, School of Applied Natural Science, Adama Science and Technology University, P O Box 1888, Adama, Ethiopia*

[2]*Department of Applied Biology, School of Applied Natural Sciences, Adama Science and Technology University, P O Box: 1888, Adama, Ethiopia*

Article Info

Article History:
Received 27 July 2020
Received in revised form 29 September 2020
Accepted 10 October 2020

Keywords:
Medicinal plants
Green synthesis
Syzygium guineense (Willd.) DC
SyG-Ag NPs
Antibacterial activity

Abstract

The medicinal plant, *Syzygium guineense* (Willd.) DC mediated green silver nanoparticles (*SyG*-Ag NPs) were successfully synthesized for the first time in Ethiopia. The synergistic influence of biomolecules of the plant leaf extract such as alkaloids, phenolic compounds, tannins, saponins and glycosides with Ag NPs towards the antibacterial activity has been investigated. The synthesized nanoparticles were characterized by UV-Vis, UV-DRS, FT-IR, XRD, SEM, EDXA, TEM, HRTEM and SAED techniques. The presence of absorbance maxima, λ_{max} at 452 nm confirms the formation of *SyG*-Ag NPs. The energy gap, E_g of NPs, was found to be 2.1 eV. FTIR spectra confirmed the presence of biomolecules in the extract and NPs. The presence of 4 sharp peaks in the XRD pattern of NPs confirmed highly crystalline nature of NPs. The purity of the NPs was confirmed by SEM-EDAX analysis. The average particle size of NPs was found to be 27.62 nm. TEM-HRTEM-SAED analysis resulted in d-spacing values of 0.2396 nm which corresponds to Ag (111) lattice fringes of *SyG*-Ag NPs. The d-spacing value of the derived diffraction planes from 4 major spots; d_{111}Ag = 0.2428 nm, d_{200}Ag = 0.2056 nm, d_{220}Ag = 0.1483 nm and d_{311}Ag = 0.1263 nm, are in agreement with the XRD data. The antibacterial test results showed synergistic effect against both Gram positive bacteria, *S. aureus* (11±0.04*mm),* and Gram negative bacteria *E. coli* (12±0.012 *mm), P. aeruginosa (10*±0.1 *mm),* and *E. aerogenes* (13±0.032 *mm),* respectively, proving potentiality of SyG-Ag NPs as a remedy for infectious diseases caused by tested pathogens.

1. Introduction

Ethiopia is one of the six centers of biodiversity in the world with 6,500 species of higher plants where traditional medicine plays a significant role and vast majority of population lives in rural areas with little access to health services (Gebrehiwet Tesfahuneygn and Gebremichael Gebreegziabher, 2019). In recent years numerous Ethiopian medicinal plants have been validated in a scientific empirical framework through phytochemical analysis and subsequent bioassays (Judžentienė, 2016). The medicinal plants species are used to treat many diseases in Ethiopia (Balcha Abera, 2014). *Syzygium guineense* (Willd.) DC is a medium-sized or tall evergreen tree, 15 - 30 m high. Its Amharic name is 'dokma', whereas, in English it is called by several names such as water pear, water boom and water berry. The ripe fruits are edible by humans, birds, and some wild animals.

* *Corresponding author, e-mail: tegened@yahoo.com and anandkps350@gmail.com*

https://doi.org/10.20372/ejssdastu:v8.i1.2021.265

© 2020 Adama Science & Technology University. All rights reserved

In southern Ethiopia *S. guineense* is a much-appreciated shade tree for both the homestead and the home garden.

The research on the fabrication of plant mediated Ag NPs for biomedical, environmental and agricultural applications has been in the forefront for the last few years. The green Ag NPs have been used for photocatalytic, electrocatalytic, organic dye degradation, biomedical, pharmaceutical, cosmetic, energy and catalytic applications since many decades (Ananda Murthy and Prakash, 2020). These Ag nanostructures such as nanoparticles, nanocrystals, nanorods, nanotubes, nanosheets exhibit versatile properties and hence found to exhibit inhibitory activity against many microorganisms and bacterial strains (Hemmati et al., 2020). A very few medicinal plants such as *Azadirachta indica* (Ahmed et al. 2016), *Dioscorea bulbifera* (Ghosh et al., 2015), *Barleria prionitis* (Sougata et al. 2016), *Caesalpinia bonducella* (Saranya Sukumar and Agneeswaran Rudrasenan, 2020), *Hagenia abyssinica* (Murthy et al., 2020) have been applied to synthesize silver, gold, copper and their oxides in the recent past for multifunctional applications. But no significant work has been done especially with the application of biomolecules of medicinal plant extracts as reducing and capping agents for the synthesis of Ag NPs in Ethiopia for biomedical, photocatalytic, electrochemical sensor and antibacterial applications.

In this work, a simple and eco-friendly green synthesis of Ag nanoparticles using medicinal plant *Syzygium guineense (SyG)* leaf extract at low temperature was proposed to investigate synergistic influence of phytochemicals and Ag NPs on bacterial strains. The synthesised *SyG*-Ag NPs have been characterised by UV-Vis, UV-DRS, FT-IR, XRD, SEM, EDXA, TEM, HRTEM and SAED techniques and investigated for their *in vitro* antibacterial activity.

2. Materials and Methods

2.1. Materials and reagent

All the chemicals, $AgNO_3$, ethanol, Dimethyl sulfoxide (DMSO) used in the experiments were of analytical grade (purchased from Merck chemical Industrial Company) and used without any further purification.

2.2. Collection and Authentication of Plant Materials

Syzygium guineense (Willd.) DC plant leaves were collected from the Arsi zone, Ethiopia. The identification of the plant *Syzygium guineense* (Voucher code EB006) was performed at the National Herbarium, Department of Biology, Addis Ababa University, Addis Ababa, Ethiopia.

2.3. Preparation of Plant Leaf Extract

The leaves of *Syzygium guineense* were surface cleaned and washed repeatedly with tap water followed by distilled water to remove dust particles and then allowed to dry under shadow for 15 days to remove moisture contents from the leaves. This procedure has been adapted from the previously published work (Murthy et al., 2020). The dried leaves were ground using grinding machine followed by packing in a brown bottle. The extraction was carried out by taking 20 g of powdered leaves of *Syzygium guineense* in a 500 ml of conical flask containing 400 ml of deionized water. The flask was later covered with aluminum foil, to prevent the effect of light. After that the mixture was shaken using mechanical shaker for 90 min. and allowed to warm at 50°C for 1 hr. on magnetic stirrer, then it was allowed to cool down to room temperature overnight. The prepared solution was filtered through whatman No.1 filter paper to get clear solution. The filtrate was stored at 4°C for future experiments.

2.4. Green Synthesis of SyG-Ag NPs

A 0.2 M aqueous $AgNO_3$ solution was prepared and stored in brown bottles. 100 ml of leaf extract was mixed with 400 ml of 0.2 M $AgNO_3$ solution (1:4) slowly dropwise with constant stirring (Kumar et al., 2019).

The mixture has been incubated at room temperature for 24 hrs. The change in color from blue to light brownish visually indicates the formation of Ag NPs and then the solution was centrifuged for 15 min at 10000 rpm. The obtained *SyG*-Ag NPs were washed thrice by deionized water and ethanol to remove any impurities. Thereafter, the NPs were allowed to dry and ground so as to be used for further analysis (Murthy et al., 2018).

2.5. Characterization Techniques

The UV-Vis absorbance and reflectance spectra of the samples were recorded in the range of 200–800 nm using Shimadzu's UV-2600, UV-vis spectrophotometer. The Ag nanoparticle solution was prepared by mixing the freshly prepared plant extract solution with Ag solution

after appropriate dilution. *Fourier* transform-infrared spectroscopy (FT-IR) Spectrum (65 FT-IR PerkinElmer) was recorded using KBr pellets in the range of 400–4000 cm^{-1}. X-ray diffraction (XRD-Shimadzu x-ray diffractometer (PXRD-7000) analytical technique was used to reveal the crystalline nature of g-Cu NPs.

The scanning electron microscopy with energy-dispersive X-ray spectroscopy (SEM-EDX-EVO 18 model with low vacuum facility and ALTO 1000 Cryo attachment) and transmission electron microscope with high-resolution (JEOL JEM 2100 HRTEM) were used for understanding morphological and structural features of *Sy*G-Ag NPs (Kumar et al., 2020). Gatan Digital Micrograph Software was used to evaluate the d-spacing values of lattice fringes. Particle size was computed by using imageJ application.

2.6. Method of Antibacterial Evaluation

All the antibacterial tests were conducted at Oromia Public Health Research, Capacity Building & Quality Assurance Laboratory, Adama, Ethiopia. The in-vitro antibacterial activity of SyG-Ag NPs was evaluated using Agar disc-diffusion method against selected one Gram positive bacterial strain (*Staphylococcus aureus*) and three Gram negative pathogenic bacterial strains (*Escherichia coli, Pseudomonas aeruginosa* and *Enterobacter aerogenes*). Prior to antibacterial activity test, the bacterial strains were cultured in nutrient broth for 24 hrs to obtain logarithmic growth phase of the test bacteria. A standardized inoculum of the bacteria is swabbed onto the surface of Mueller-Hinton Agar (MHA) plate. The actively growing bacterial cultures of 1.3×10^8 CFU/mL concentration were inoculated/spread onto the MHA plate (turbidity was adjusted with TSB to match 0.5 McFarland standard). The nanoparticles extract was prepared with four different concentrations in Dimethyl Sulfoxide. Four concentrations (6.25, 12.5, 25 and 50 µg/µl) of the synthesized nanoparticles were added to the respectively labeled wells.

The antibiotic discs of 6 mm diameter were applied to agar surface using forceps with gentle pressure and then impregnated with the dissolved extract. Chloramphenicol disc was used as a positive control while DMSO was taken as negative control. The plates were incubated at 35 ±2°C in an ambient air incubator for 18-24 hrs. The antibacterial activity was evaluated in terms of zone of inhibition, measured to the nearest millimeters (mm) using a ruler and recorded.

3. Results and Discussions

3.1. Synthesis of *Sy*G-Ag NPs

The *Sy*G-Ag NPs were synthesized by using silver nitrate as a precursor and *Syzygium guineense* (Willd.) DC plant leaf extract as a reducing and capping agent. The presence of alkaloids, phenolic compounds, tannins, saponins, anthraquinone glycosides and cardiac glycosides was confirmed during the phytochemical screening of *Syzygium guineense* leaf extract. The details of the phytochemicals present in the extract are as given in Table 1. Three stages of formation of NPs includes: reduction of metal ions, formation of cluster and growth of nanoparticles. It is learnt that the tautomeric transformation of polyphenols from enol form to keto form would release reactive hydrogen atom that reduces silver ions to silver nanoparticles. In addition, the enzymes of leaf extract also assist silver ions to form an enzyme substrate complex resulting into formation of protein capped silver NPs (Roy et al., 2019). It is also understood that the phenolic compounds act as ligand and bind to metal ions and reduce them and cap them to form nanoparticles. These ligands also act as particle size controllers as reported by the earlier researcher (Azarbani & Shiravand, 2020).

Table 1: The details of phytoconstituents screening of *Syzygium guineense* plant leaves extract.

Sl. No.	Phytoconstituents	Test / Reagent	Result
1	Alkaloids	Wagner's reagent	+
2	Tannins	KOH	+
3	Flavonoids	Shinoda Test	-
4	Terpenoids	Salkowski Test	-
5	Anthraquinone glycosides	Borntrager's Test	+
6	Cardiac glycosides	Keller-Kiliani Test	+
7	Saponins	Frothing Test	+
8	Phenols	$FeCl_3$	+

'+' indicates the presence and '-' indicates the absence

Primary components of *Syzygium guineense* extract are alkaloids, phenolic compounds, tannins, saponins, anthraquinone glycosides and cardiac glycosides. The antioxidant properties of phenolic compounds are primarily due to their high inclination towards chelating the metals. Phenolic compounds contain hydroxyl and carboxylic groups which have very high tendency to bind metal ions. Metal ions in solution interact with phenolic compounds which help in the nucleation and formation of Ag NPs.

3.2. Characterization of *Sy*G-Ag NPs

The *Sy*G-Ag NPs were characterized using UV-Vis, UV-DRS, FT-IR, XRD, SEM, EDXA, TEM, HRTEM and SAED techniques.

3.2.1. UV-Vis spectral analysis

The UV-Vis absorbance spectrum recorded for instantaneously synthesized *Sy*G-Ag NPs exhibited λ_{max} of 452 as shown in Figure 1a, just after 10 min of mixing plant extract with copper nitrate solution in 1:4 ratios.

This absorption band is basically due to surface plasmon resonance of *Sy*G-Ag NPs. The absorbance spectrum recorded after 30 min of forming NPs, exhibited another identical absorbance band at λ_{max} of 452 nm (Figure 1b). The enhanced absorbance in the 2nd band, clearly confirm the increased concentration of NPs. As the time proceeds on, the reduction of copper ions is followed by nucleation of small cluster of copper atoms to form nanoparticles in the presence of biomolecules of plant extract which are possibly believed to have acted as reducing agent and stabilizing agent. Poly phenolic compounds usually help in the reduction of silver ions into silver atoms which form cluster and nanoparticles at the later stage.

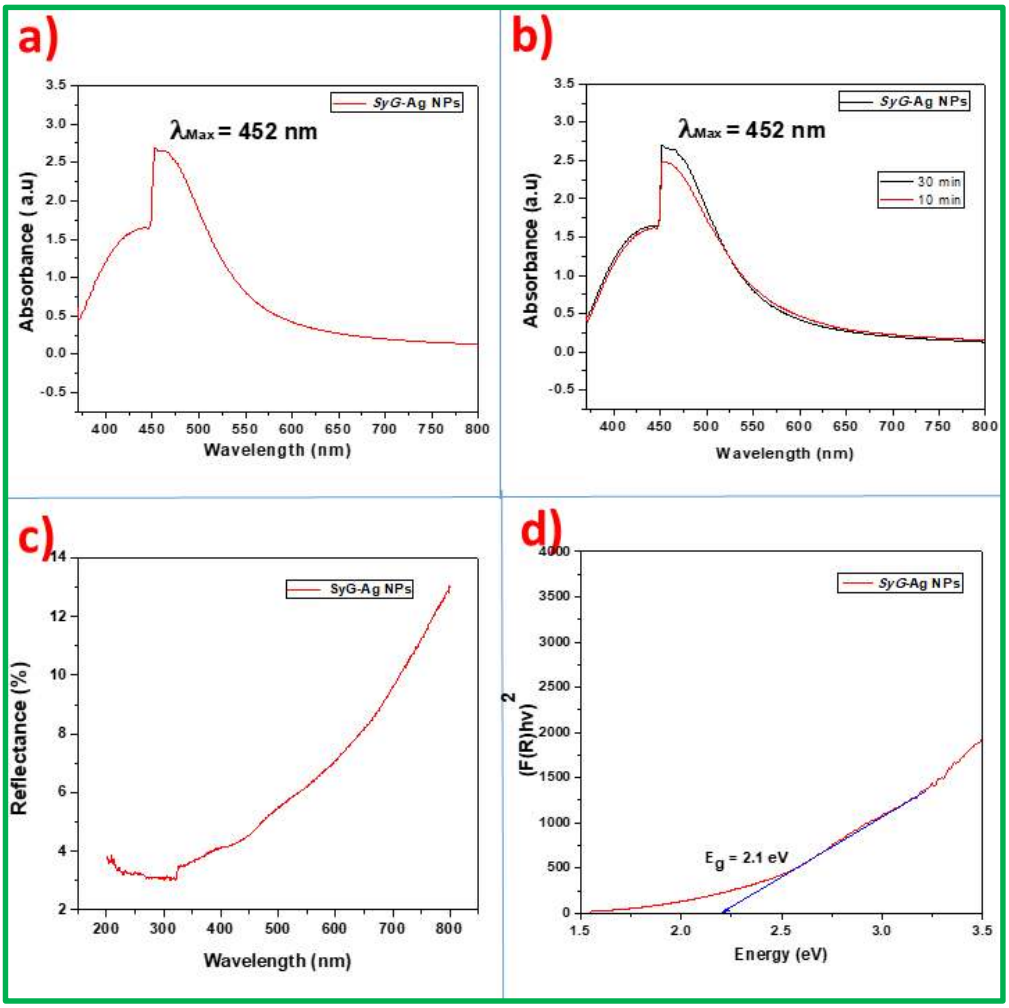

Figure 1: (a) and (b) UV-Vis absorbance spectrum of *Sy*G-Ag NPs at different time intervals (c) UV-Vis diffused reflectance spectrum of *Sy*G-Ag NPs. (d) Tauc plot of *Sy*G-Ag NPs showing Eg Value.

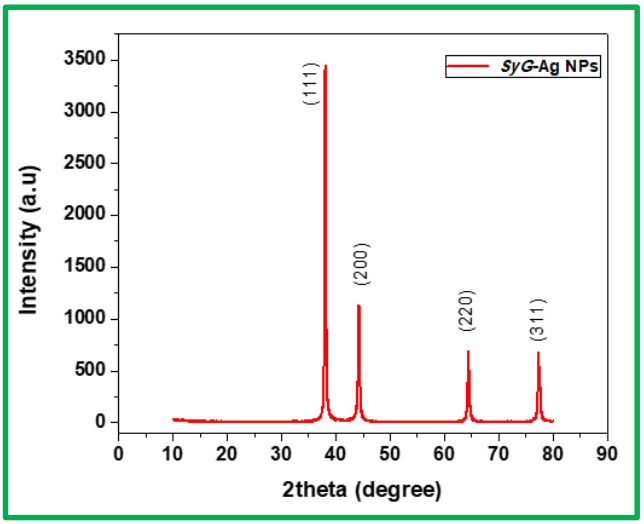

Figure 2: The XRD pattern of *Sy*G-Ag NPs.

A similar result was reported after the analysis of synthesized Ag NPs by using the *Lustrum lucidum leaf* extract (Huang et al., 2020) and *Persea americana* seed extract (Girón-Vázquez et al., 2019). The surface plasmon absorbance presents a set of different λ_{max} values for NPs synthesised using different plant extracts which is possibly due to morphological features of the NPs. Similarly, the UV-Vis diffused reflectance spectrum was recorded (Figure 1c). The band gap energy of *SyG*-Ag NPs was evaluated using Tauc plot as shown in figure 1d by using the data obtained in reflectance spectra utilizing Kubelka-Munk function. The band gap energy, E_g of *SyG*-Ag NPs was found to be 2.1 eV.

3.2.2. XRD analysis

The XRD diffraction pattern of *SyG*-Ag NPs is presented in figure 2. The peaks at 2θ values = 38.14°, 44.72°, and 64.50°, and 77.42° corresponds to (111), (200), (220) and (311) lattice planes of face centred cubic structure of Ag NPs and the diffraction results were in good agreement with the data of ICPD file no. 00-004-7383 (Fm3m) (Sadeghi & Gholamhoseinpoor, 2015).

3.2.3. FT-IR spectral analysis

The FTIR spectra of *SyG* plant extract and *SyG*-Ag NPs is presented in figure 3. FTIR spectra confirmed the presence of biomolecules in the extract and NPs. The broad peaks appeared in the region between 3391 and 2926 cm^{-1} corresponds to –OH stretching vibration and sp^3 C-H stretching vibrations, respectively. The peak at 1623 cm^{-1} corresponds to C=O stretching of carbonyl groups. The sharp peak around 1450 cm^{-1} shows the presence of −COO group of carboxylic acid. It is also believed that the amine and carboxylate group present in the *SyG* plant leaf extract responsible for the binding of proteins with the surface of Ag and thereby leading to the stabilization of the biosynthesized nanoparticles.

The peaks represented by 1350 cm^{-1} shows C-N stretching of amide. The medium peak at 1160 cm^{-1} corresponds to C-O stretching of phenolic compounds. The C-O-C stretching appears at 1038 cm^{-1}. The bending vibrations of Ag–O–H bonds resulted in a small peak at 800 cm^{-1} which can be attributed to the presence of the Ag–O bond. The last peak at 665 cm^{-1} corresponds to bending modes of vibrations of C–H bond. The small shift in the IR bands indicates the possible reaction of silver ions and synthesis of nanoparticles in the extract. FTIR analysis results confirmed the presence of various phytochemicals of *Syzygium guineense* leaf extract such as alkaloids, phenolic compounds, tannins, saponins, anthraquinone glycosides and cardiac glycosides involved in the synthesis of SyG-Ag NPs.

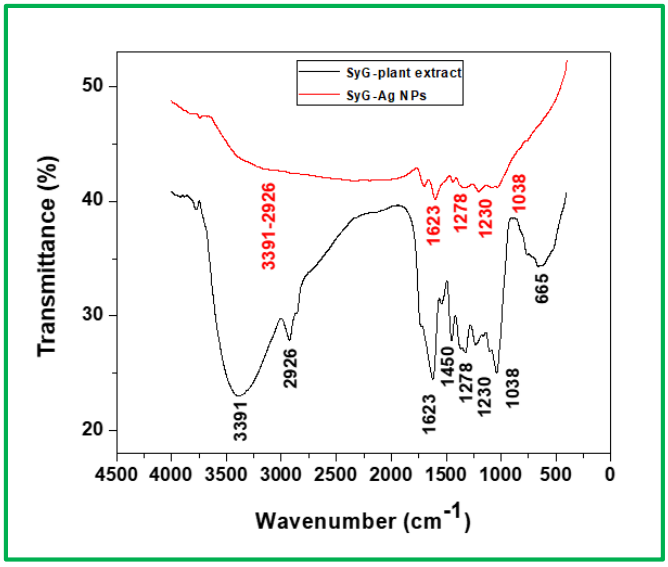

Figure 3: The FTIR spectra of *Sy*G plant extract and *Sy*G-Ag NPs.

3.2.4. Morphological and compositional analysis by SEM-EDAX

The morphological features of synthesized *SyG*-Ag NPs as depicted by SEM micrographs are shown in figure 4a and 4b. The SEM images also depicted

varieties of nanosized particles with diversified size ranges as well as shapes. All the possible nearly spherical and diverse shapes such as hexagonal, cylindrical, triangular and prismatic shapes of Ag NPs with varying particle sizes were found in the micrographs. The average grain size of Ag NPs was found to be in the range between 10 and 40 nm (Velgosova et al., 2019).

The presence of less agglomerated Ag NPs possibly due to moderate surface area which yielded small sized particles. The Ag NPs were found to be as small as 10.1 nm in their dimension which clearly confirms the efficient role of biomolecules as stabilizing agents preventing the growth of clusters of silver atoms to bigger NPs. The chemical composition of the NPs was studied by EDAX analysis. Figure 4c shows the EDAX spectrum obtained for the *SyG*-Ag NPs. The peaks corresponding to elemental Ag, C and Cl were clearly identified and additional peak for Au appeared due to the usage of standard during the analysis.

It is also possibly believed that the presence of C is basically from the capped bioactive compounds. The reduction of silver ions to Ag NPs is facilitated by the biomolecules of plant extract containing surface hydroxyl groups.

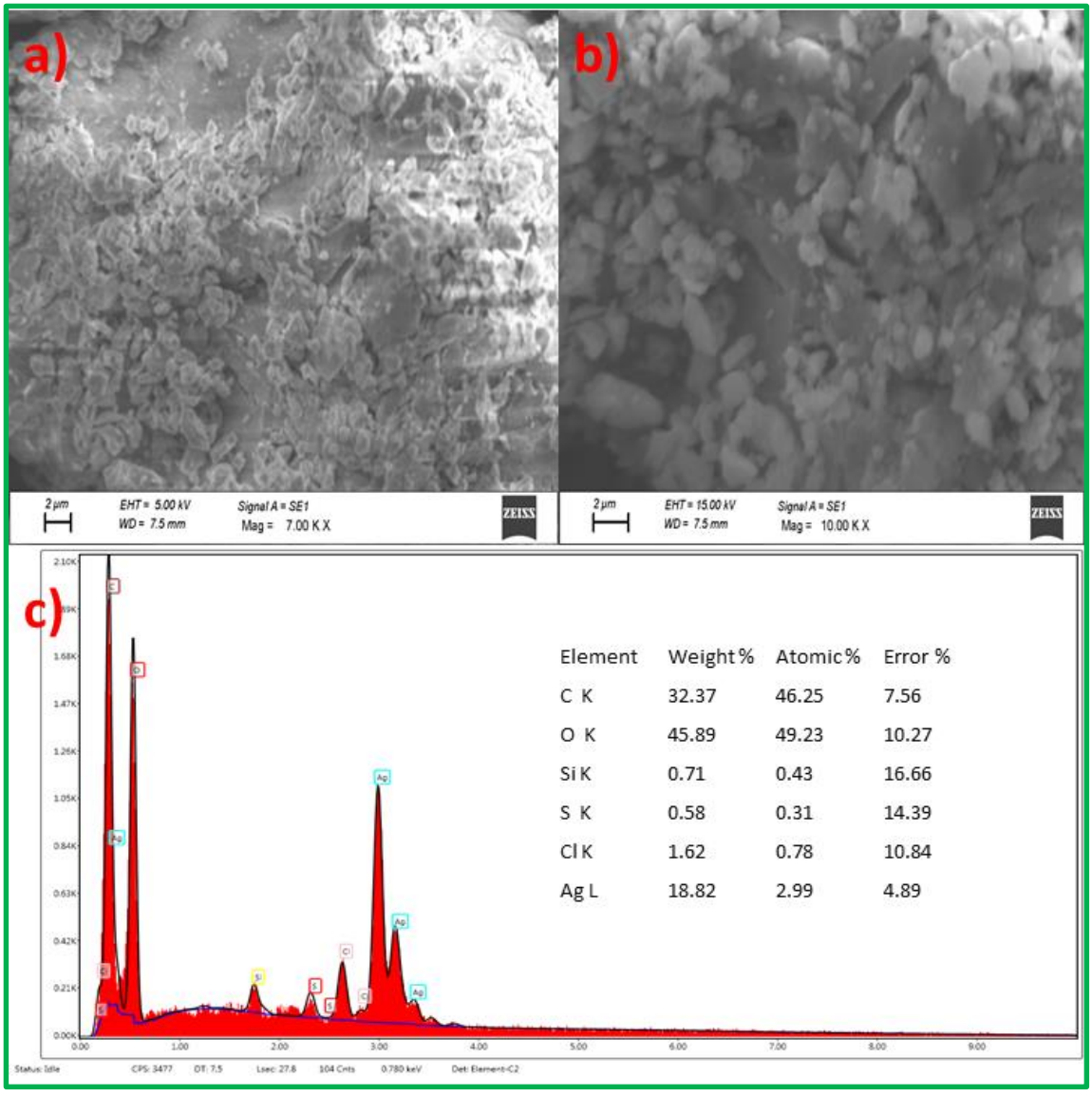

Figure 4: (a) and (b) SEM micrographs of *VeA*-Ag NPs (c) EDAX spectrum of *Sy*G-Ag NPs.

3.2.5. TEM, HRTEM and SAED analysis

In order to explore deep insights into the morphological and structural features of the *Sy*G-Ag NPs, TEM, HRTEM and SAED technical micrographs and patterns were utilized. The HRTEM images of as-synthesized *Sy*G-Ag NPs (Figure 5) shows that the synthesized NPs are nearly spherical but exhibited varieties of shapes.

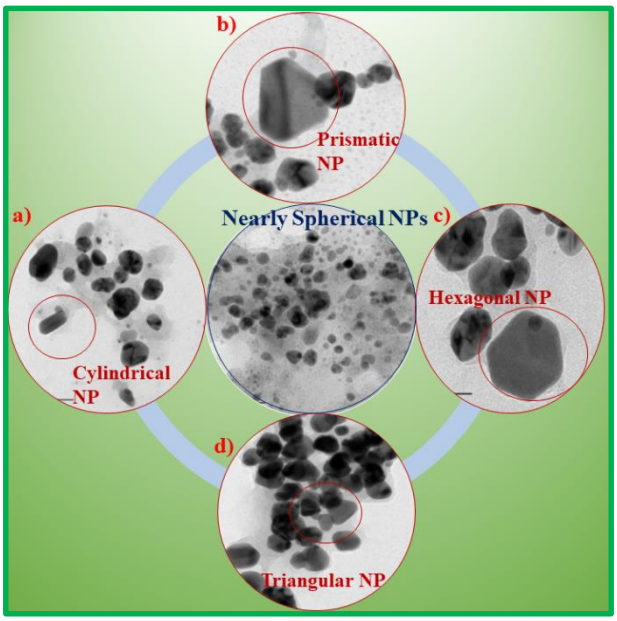

Figure 5: The TEM micrographs showing *Sy*G-Ag NPs with a) cylindrical, b) prismatic c) hexagonal, and d) triangular shapes with nearly spherical shapes.

The smaller NPs as small as 10.1 nm confirm the efficient role of bioactive components of *Syzygium guineense* plant extract as capping and stabilizing agents. Otherwise NPs would have been agglomerated to yield larger NPs in an elongated form.

In addition, the variation in size of *SyG*-Ag NPs is probably due to the presence of polyphenolic compounds which have strong attractive forces and holds the particles together.

The TEM micrographs which exhibited very finely grained *SyG*-Ag NPs with cylindrical, prismatic, hexagonal, triangular shapes as well as nearly spherical shapes are presented in Figure 5a to 5d.

The nearly spherical particles with varying sizes from 10.1 nm to 54.7 nm with an average particle size of 27.62 nm as determined by image J application are as shown in Figure 6a and 6b.

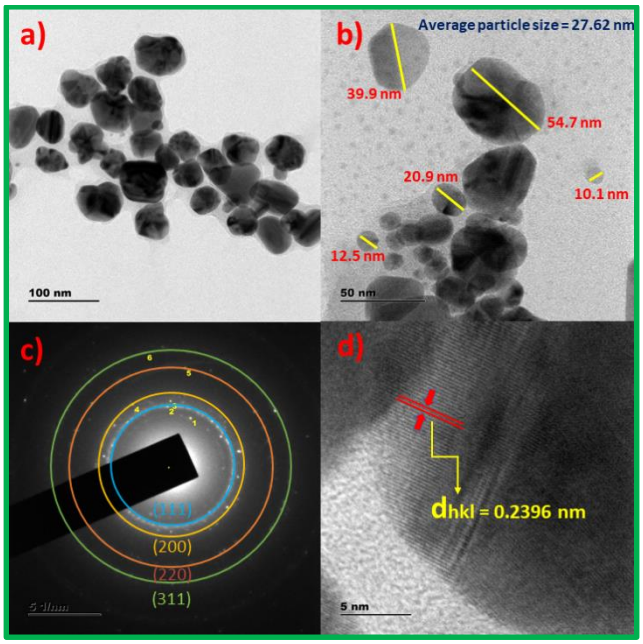

Figure 6: TEM images of as-synthesized *Sy*G-Ag NPs at (a) lower magnification (100 nm) and (b) higher magnification (50 nm) (c) SAED pattern with 1 to 6 spots and (d) HRTEM image showing lattice fringes of *Sy*G-Ag NPs with d-spacing of 0.2396 nm.

The SAED pattern of *SyG*-Ag NPs (Figure 6c) contained six spots each corresponding to specific crystal planes. The most prominent 4 spots were represented in colored concentric circles which represents (111), (200), (220) and (311) planes. The d-spacing of 0.2396 nm for Ag (111) plane is as shown in Figure 6d. HRTEM morphology of *SyG*-Ag NPs with magnified lattice fringes, IFFT patterns and profile of IFFT with d-spacing value for Ag (111) plane (Figure 6d) are presented in Figure 7a, 7b, 7c and 7d respectively. The image analysis to arrive at d-spacing value has been carried out by using Gatan Digital Micrograph Software application which resulted in d_{hkl} value of 0.2396 nm a set of crystal planes at the surface of Ag NPs.

The d-spacing values for the most prominent four spots depicted in the SAED pattern of *SyG*-Ag NPs (Figure 6c) are presented in Table 2. Each spot on the SAED pattern corresponds to specific set of lattice planes. The XRD pattern of NPs presented earlier in Figure 3, revealed 4 major peaks corresponding to (111), (200), (220) and (311) planes of fcc structure of pure Ag (ICPD file no. 00-004-7383 (Fm3m)). The d-spacing

Table 2: The d-spacing values for *Sy*G-Ag NPs from SAED pattern.

Spot No.	d- spacing (nm)	Rec. Pos. (1/nm)	Degrees to Spot 1	Degrees to x- axis	Amplitude
1	0.2428	4.145	0.00	80.37	2839.10
2	0.2126	4.678	2.04	78.33	4168.58
3	0.2056	4.895	52.10	28.27	4484.95
4	0.1483	6.756	6.11	74.26	1295.65
5	0.1263	7.954	5.87	86.24	5564.48
6	0.09527	10.40	19.92	60.45	4062.21

values of the derived diffraction planes corresponding to spots 1, 3, 4 and 5; d_{111}Ag = 0.2428 nm, d_{200}Ag = 0.2056 nm, d_{220}Ag = 0.1483 nm and d_{311}Ag = 0.1263 nm, are in agreement with the standard d-spacing values of Ag (ICPD file no. 00-004-7383 (Fm3m)) structure.

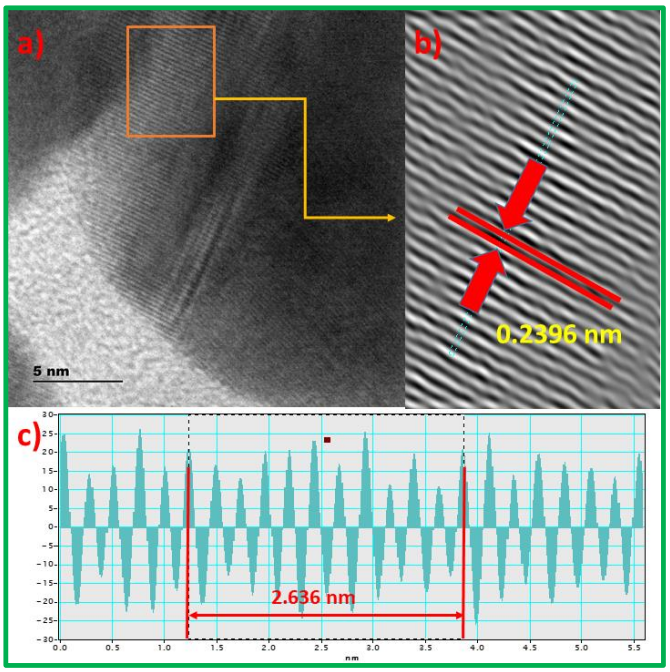

Figure 7: HRTEM morphology of *Sy*G-Ag NPs (a) Magnified lattice fringes (b) IFFT patterns (c) Profile of IFFT with d-spacing distance.

3.3. Antibacterial Activity

The *SyG*-Cu/Cu_2O/CuO NPs exhibited broad range of antibacterial activities against all tested pathogens; *S. aureus, E. coli, P. aeruginosa,* and *E. aerogenes.* The present work evaluated synergistic influence of biomolecules with NPs against 4 pathogens. The zone of inhibitions for Chloramphenicol, DMSO and NPs with four concentrations (6.25, 12.5, 25 and 50 µg/µl). Pure Ag NPs were proved to exhibit excellent anti*bacterial* activity. Accordingly, *SyG*-Ag NPs were found to show better anti*bacterial* activity against Gram positive bacteria than Gram negative bacteria which is believed to be due to the structural differences in the cell walls of bacteria (Abebe et al., 2020).

SyG-Ag NPs were found to show better antibacterial activity against Gram negative bacteria than Gram positive bacteria which is believed to be due to the structural differences in the cell walls of bacteria. The antibacterial activity of NPs can be partially attributed to the presence of bioactive compounds on the surface of NPs as capping and stabilizing agents. In this regard, the activity was pronounceable against *S. aureus*. The highest zone of inhibition (mm) recorded with 50 µg/µl of *SyG*-Ag NPs against *E. aerogenes* bacteria was 13±0.032 mm and the lowest zone of inhibition (mm) recorded against P. *aeruginosa* bacteria was 10±0.1 mm (Table 3).

The wide zone of inhibitions of *SyG*-Ag NPs against pathogens confirm their great potentiality as a remedy for infectious diseases caused by the tested bacterial pathogens.

Additionally, the standard disc Chloramphenicol showed comparable zone of inhibition with the *SyG*-Ag NPs, which is small and it can be attributed to development of resistance by bacteria against Chloramphenicol. The zone of inhibition values for *SyG*-Ag NPs was found to be moderately lower for *S. aureus, E. coli* and *E. aerogenes* except *P. aeruginosa* when compared with that of positive control Chloramphenicol. It is mainly due to the differences in the chemical structure of the bacterial cell walls and as a consequence different types of interactions occur between differently sized NPs and bacterial strains. The interaction between Ag NPs and microorganisms starts with adhesion of Ag NPs to the microbial cell wall and membrane, which is based on electrostatic attraction between the negatively charged microbial cell membrane and positively or less negatively charged Ag NPs. Zeta potential is another physico-chemical property influence antimicrobial activity since the interaction between NPs

Table 3: The variation of zone of inhibitions for different bacteria by *Sy*G-Ag NPs.

Concentration of NPs (µg/µL)	Bacterial strains and Zone of Inhibition in mm			
	S. aureus ATCC25923	*E. coli* ATCC25992	*P. aeruginosa* ATCC27853	*E. Aerogenes* ATCC13048
50	11±0.04	12±0.012	10±0.1	13±0.032
25	11±0.005	10±0.06	8±0.05	10±0.103
12.5	6±0.008	8±0.017	6±0.057	8±0.007
6.25	6±0.11	6±0.002	6±0.043	6±0.041
Chloramphenicol	24±0.14	20±0.015	6±0.001	30±0.016
DMSO	6±0.006	6±0.02	6±0.003	6±0.01

Table 4: Comparative data of antibacterial activities of Ag NPs synthesised by using various plant extracts.

Sl. No.	Plant extract	Zone of Inhibition (mm)	Tested Pathogens	Reference
1	*Bergenia cili*(Phull et al., 2016) *ata*	8.5	*S. aureus*	(Phull et al. 2016)
2	*Balloon flower plants*	12	*E. coli*	(Anbu et al., 2019)
3	*Aloe fleurentiniorum*	12, 14.5	*E. coli, S. aureus*	(Salmen & Alharbi, 2020)
4	*Chenopodium murale*	12.7	*S. aureus*	(Abdel-Aziz et al., 2014)
5	*Syzygium guineense*	11, 12, 10, 13	*S. aureus,* *E. coli,* *P. aeruginosa,* *E. aerogenes.*	Present work
6	*Ocimum Sanctum (Tulsi)*	14	*E.coli*	(Jain & Mehata, 2017)
7	*Citrus paradisi (grapefruit red)*	22	*E.coli*	(Ayinde et al., 2018)
8	*Coffea arabica*	23, 21	*E. coli, S. aureus*	(Dhand et al., 2016)
9	Banana peel extract	17, 20, 16, 12	*E. coli,* *P. aurognosa,* *S. aureus,* *B. subtilis.*	(Ibrahim, 2015)
10	*Allium cepa*	24, 23, 25	*E. coli,* *S. aureus,* *B. subtilis.*	(Gomaa, 2017)
11	*Rosmarinus officinali*	17.2, 18.8, 31.2, 16.2	*E. coli,* *P. aurognosa,* *S. aureus,* *B. subtilis.*	(Khafri, 2015)
12.	*Cassia roxburghii leaf*	33	*E. coli*	(Moteriya et al., 2017)

and the cell membrane is based on electrostatic adhesion which is different for different bacterial strains.

Furthermore, Ag NPs could interact with protein parts of the outer membrane of bacterial strain, constitute complexes with oxygen, phosphorous, nitrogen or sulphur atom containing electron donors, and cause irreversibly changes in the cell wall structure. The moderate zone of inhibitions exhibited by the *SyG*-Ag NPs is possibly because of the application of very small amounts of NPs compared to the amount of NPs utilized by various researchers.

Many mechanisms of antibacterial activity have been reported by the past researchers, accordingly, the action of *SyG*-Ag NPs on the bacteria is yet to be explored fully. It is assumed that the *SyG*-Ag NPs get adsorbed on to the cell wall of bacteria and interacts with the electronegative elements within the cell membrane.

These results in failed metabolism and thereby leading to interference and disruption of transcription in bacteria and hence causes antibacterial activity by *SyG*-Ag NPs. It is also believed that the synergistic effect of *SyG*-Ag NPs with bioactive compounds of extract would have played significance influence to inhibit the activity of pathogenic bacteria.

The anti*bacterial* results obtained using *SyG*-Ag NPs were found to be better when compared with an earlier

work reported by many researchers (Table 4). The highest zone of inhibition (mm) recorded with *SyG*-Ag NPs against *E. aerogenes* bacteria was 13±0.032 mm which is higher than the zone of inhibition exhibited by Ag NPs synthesized by various plant extracts as mentioned in Table 4. The last few plant extracts were proved to exhibit a higher zone of inhibition which can be attributed to the presence of different type of phytoconstituents.

Another possible mechanism of the inhibitory phenomenon was that the cell walls of Gram-positive bacteria bound larger quantities of metal (Ag) than Gram-negative bacteria. Most studies have shown that Gram-negative bacterial growth is more affected by Ag NPs than Gram-positive bacteria which can be attributed to thin cell walls that are easily penetrated, while Gram-positive bacteria have thicker cell wall (Anbu et al., 2019). It is possibly understood that the helical structure of DNA molecules would have disrupted by the action of *SyG*-Ag NPs. In addition, electrochemical potential across the cell membrane decreases up on interaction with the released Ag metal ion by *SyG*-Ag NPs affecting integrity of the membrane.

4. Conclusion

The application of medicinal plant, *Syzygium guineense* leaf extract towards the green synthesis of silver (*SyG*-Ag) nanostructures was successful. The UV-Vis spectra, XRD pattern and FTIR spectra confirmed the formation of crystalline SyG-Ag NPs in the presence of biomolecules such as ploy phenolics, tannins, glycosides and proteins of the plant extract. SEM and TEM micrographs of *SyG*-Ag NPs revealed cylindrical, prismatic, hexagonal, triangular and spherical morphologies. HRTEM-SAED analysis confirmed the presence of crystalline Ag by the observation of Ag (111), (200), (220) and (311) lattice fringes in *SyG*-Ag NPs with the calculated d-spacing values matching exactly with the standard value for Ag. The *SyG*-Ag NPs are identified as effective anti*bacterial* agents against multiple microbes of various strains. The synergistic influence of bioactive compounds, *SyG*-Ag NPs and antibiotic ampicillin proved to be highly effective against pathogens, Gram-positive and Gram-negative bacterial strains *S. aureus, E. coli, P. aeruginosa,* and *E. aerogenes.* It is expected that this accomplished work will initiate research towards the green synthesis of fabricated metallic nanoparticles for prospective biomedical applications.

Acknowledgments

This work has been funded by the project (ANSD/04/0453/11-2018) approved by the Research and Technology Transfer Office, sanctioned by Adama Science and Technology University, Ethiopia. The authors gratefully acknowledge Adama Science and Technology University for the financial support and laboratory facility to conduct this research work.

Reference

Abdel-Aziz, M. S., Shaheen, M. S., El-Nekeety, A. A., & Abdel-Wahhab, M. A. (2014). Antioxidant and antibacterial activity of silver nanoparticles biosynthesized using Chenopodium murale leaf extract. *Journal of Saudi Chemical Society*, *18*(4): 356–363. https://doi.org/10.1016/j.jscs.2013.09.011

Abebe, B., Murthy, H. C. A., Zerefa, E., & Adimasu, Y. (2020). PVA assisted ZnO based mesoporous ternary metal oxides nanomaterials: synthesis, optimization, and evaluation of antibacterial activity. *Materials Research Express*, *7*(4): 045011. https://doi.org/10.1088/2053-1591/ab87d5

Abera, B. (2014). Medicinal plants used in traditional medicine by Oromo people, Ghimbi District, Southwest Ethiopia. *Journal of Ethnobiology and Ethnomedicine*, *10*(1). https://doi.org/10.1186/1746-4269-10-40

Ahmed, S., Saifullah, Ahmad, M., Swami, B. L., & Ikram, S. (2016). Green synthesis of silver nanoparticles using Azadirachta indica aqueous leaf extract . *Journal of Radiation Research and Applied Sciences*, *9*(1): 1–7. https://doi.org/10.1016/j.jrras.2015.06.006

Anbu, P., Gopinath, S. C. B., Yun, H. S., & Lee, C. G. (2019). Temperature-dependent green biosynthesis and characterization of silver nanoparticles using balloon flower plants and their antibacterial potential. *Journal of Molecular Structure*, *1177*, 302–309. https://doi.org/10.1016/j.molstruc.2018.09.075

Ayinde, W. B., Gitari, M. W., Muchindu, M., & Samie, A. (2018). Biosynthesis of Ultrasonically Modified Ag-MgO Nanocomposite and Its Potential for Antimicrobial Activity. *Journal of Nanotechnology*, *2018:* 1–10. https://doi.org/10.1155/2018/9537454

Azarbani, F., & Shiravand, S. (2020). Green synthesis of silver nanoparticles by Ferulago macrocarpa flowers extract and their antibacterial, antifungal and toxic effects. *Green Chemistry Letters and Reviews*, *13*(1): 41–49. https://doi.org/10.1080/17518253.2020.1726504

Dhand, V., Soumya, L., Bharadwaj, S., Chakra, S., Bhatt, D., & Sreedhar, B. (2016). Green synthesis of silver nanoparticles using Coffea arabica seed extract and its antibacterial activity. *Materials Science and Engineering C*, *58*: 36–43. https://doi.org/10.1016/j.msec.2015.08.018

Ghosh, S., Jagtap, S., More, P., Shete, U. J., Maheshwari, N. O., Rao, S. J., Kitture, R., Kale, S., Bellare, J., Patil, S., Pal, J. K., & Chopade, B. A. (2015). Dioscorea bulbifera Mediated Synthesis of Novel Au core Ag shell Nanoparticles with Potent Antibiofilm and Antileishmanial Activity. *Journal of Nanomaterials*, *2015:* 1–12. https://doi.org/10.1155/2015/562938

Girón-Vázquez, N. G., Gómez-Gutiérrez, C. M., Soto-Robles, C. A., Nava, O., Lugo-Medina, E., Castrejón-Sánchez, V. H., Vilchis-Nestor, A. R., & Luque, P. A. (2019). Study of the effect of Persea americana seed in the green synthesis of silver nanoparticles and their antimicrobial properties. *Results in Physics*, *13*(February): 102142. https://doi.org/10.1016/j.rinp.2019.02.078

Gomaa, E. Z. (2017). Antimicrobial, antioxidant and antitumor activities of silver nanoparticles synthesized by Allium cepa extract: A green approach. *Journal of Genetic Engineering and Biotechnology*, *15*(1): 49–57. https://doi.org/10.1016/j.jgeb.2016.12.002

Ananda Murthy, H.C., Prakash, C. H., Buzuayehu. A. & Kumar S. (2020). Current Research in Science and Technology Vol. 4. In D. S. Moon (Ed.), *Current reearch in Science and Technology* (Vol. 4). Book Publisher International (a part of SCIENCEDOMAIN International). https://doi.org/10.9734/bpi/crst/v4

Hemmati, S., Harris, M. T., & Barkey, D. P. (2020). Polyol Silver Nanowire Synthesis and the Outlook for a Green Process. *Journal of Nanomaterials*, *2020:* 1–25. https://doi.org/10.1155/2020/9341983

Huang, W., Yan, M., Duan, H., Bi, Y., Cheng, X., & Yu, H. (2020). Synergistic Antifungal Activity of Green Synthesized Silver Nanoparticles and Epoxiconazole against Setosphaeria turcica. *Journal of Nanomaterials*, *2020*. https://doi.org/10.1155/2020/9535432

Ibrahim, H. M. M. (2015). Green synthesis and characterization of silver nanoparticles using banana peel extract and their antimicrobial activity against representative microorganisms. *Journal of Radiation Research and Applied Sciences*, *8*(3): 265–275. https://doi.org/10.1016/j.jrras.2015.01.007

Jain, S., & Mehata, M. S. (2017). Medicinal Plant Leaf Extract and Pure Flavonoid Mediated Green Synthesis of Silver Nanoparticles and their Enhanced Antibacterial Property. *Scientific Reports*, *7*(1): 1–13. https://doi.org/10.1038/s41598-017-15724-8

Judžentienė, A. (2016). Wormwood (Artemisia absinthium L.) Oils. In *Essential Oils in Food Preservation, Flavor and Safety, 4*(1): 849–856). Elsevier. https://doi.org/10.1016/B978-0-12-416641-7.00097-3

Khafri, H. Z. (2015). Rosmarinus officinalis leaf extract mediated green synthesis of silver nanoparticles and investigation of its antimicrobial properties. *Journal of Industrial and Engineering Chemistry*, *31:* 167–172. https://doi.org/10.1016/j.jiec.2015.06.020

Kumar, M. R. A., Abebe, B., Nagaswarupa, H. P., Murthy, H. C. A., Ravikumar, C. R., & Sabir, F. K. (2020). Enhanced photocatalytic and electrochemical performance of TiO2-Fe2O3 nanocomposite: Its applications in dye decolorization and as supercapacitors. *Scientific Reports*, *10*(1): 1249. https://doi.org/10.1038/s41598-020-58110-7

Kumar, M. R. A., Ravikumar, C. R., Nagaswarupa, H. P., Purshotam, B., Gonfa, B. A., Murthy, H. C. A., Sabir, F. K., & Tadesse, S. (2019). Evaluation of bi-functional applications of ZnO nanoparticles prepared by green and chemical methods. *Journal of Environmental Chemical Engineering*, *7*(6): 103468. https://doi.org/10.1016/j.jece.2019.103468

Moteriya, P., Padalia, H., & Chanda, S. (2017). Characterization, synergistic antibacterial and free radical scavenging efficacy of silver nanoparticles synthesized using Cassia roxburghii leaf extract. *Journal of Genetic Engineering and Biotechnology*, *15*(2): 505–513. https://doi.org/10.1016/j.jgeb.2017.06.010

Murthy, H. C. A., Abebe, B., & Z, T. D. (2018). *Material Science Research India A Review on Green Synthesis and Applications of Cu and CuO Nanoparticles*. *15*(3).

Murthy, H. C. A., Desalegn Zeleke, T., Ravikumar, C. R., Anil Kumar, M. R., & Nagaswarupa, H. P. (2020). Electrochemical properties of biogenic silver nanoparticles synthesized using Hagenia abyssinica (Brace) JF. Gmel. medicinal plant leaf extract. *Materials Research Express*, *7*(5): 055016. https://doi.org/10.1088/2053-1591/ab9252

Phull, A.-R., Abbas, Q., Ali, A., Raza, H., kim, S. J., Zia, M., & Haq, I. (2016). Antioxidant, cytotoxic and antimicrobial activities of green synthesized silver nanoparticles from crude extract of Bergenia ciliata. *Future Journal of Pharmaceutical Sciences*, *2*(1): 31–36. https://doi.org/10.1016/j.fjps.2016.03.001

Roy, A., Bulut, O., Some, S., Mandal, A. K., & Yilmaz, M. D. (2019). Green synthesis of silver nanoparticles: Biomolecule-nanoparticle organizations targeting antimicrobial activity. *RSC Advances*, *9*(5): 2673–2702. https://doi.org/10.1039/c8ra08982e

Sadeghi, B., & Gholamhoseinpoor, F. (2015). A study on the stability and green synthesis of silver nanoparticles using Ziziphora tenuior (Zt) extract at room temperature. *Spectrochimica Acta - Part A: Molecular and Biomolecular Spectroscopy*, *134:* 310–315. https://doi.org/10.1016/j.saa.2014.06.046

Salmen, S. H., & Alharbi, S. A. (2020). Silver nanoparticles synthesized biogenically from Aloe fleurentiniorum extract: characterization and antibacterial activity. *Green Chemistry Letters and Reviews*, *13*(1): 1–5. https://doi.org/10.1080/17518253.2019.1707883

Saranya Sukumar, Agneeswaran Rudrasenan, and D. P. N. (2020). Green synthesis of Cu/Cu2O/CuO nanostructures and the analysis of their electrochemical properties. *ACS Omega*, *5*(2): 1040. https://doi.org/10.1021/acsomega.9b02857

Shume, W. M., Murthy, H. C. A., & Zereffa, E. A. (2020). A Review on Synthesis and Characterization of Ag 2 O Nanoparticles for Photocatalytic Applications. *Journal of Chemistry*, *2020*: 1–15. https://doi.org/10.1155/2020/5039479

Sougata, G., & Maliyackal, Jini, Chacko,. Ashwini, N, Harke,. Sonal, P, Gurav,. Komal, A, Joshi,. Aarti, Dhepe,. Anuja, S, Kulkarni,. Vaishali, S, Shinde,. Vijay, Singh, Parihar,. Adersh, Asok,. Kaushik, Banerjee,. Narayan, Kamble,. Jayesh, Bellare,. Balu, A, C. (2016). Nanomedicine & Nanotechnology Barleria prionitis Leaf Mediated Synthesis of Silver and Gold. *Journal of Nanomedicine & Nanotechnology*, *7*(4). https://doi.org/10.4172/2157-7439.100039

Tesfahuneygn, G., & Gebreegziabher, G. (2019). Medicinal Plants Used in Traditional Medicine by Ethiopians: A Review Article OPEN ACCESS. *Journal of Genetics and Genetic Engineering*, *4*(1): 1–3.

Velgosova, O., Mrazíková, A., Veselovský, L., Willner, J., & Fornalczyk, A. (2019). Influence of different plants extracts on silver nanoparticles green synthesis. *Archives of Metallurgy and Materials*, *64*(2): 665–670. https://doi.org/10.24425/amm.2019.127596.